Available online at www.sciencedirect.com
ScienceDirect
Journal of Molecular Catalysis A: Chemical 283 (2008) 99–107
JOURNAL OF MOLECULAR CATALYSIS A: CHEMICAL
www.elsevier.com/locate/molcata

# Immobilization of metalloporphyrins into nanotubes of natural halloysite toward selective catalysts for oxidation reactions

Guilherme Sippel Machado [a], Kelly Aparecida Dias de Freitas Castro [a], Fernando Wypych [b,c], Shirley Nakagaki [a,c,*]

[a] *Universidade Federal do Paraná, Departamento de Química, Laboratório de Bioinorgânica e Catálise, CP 19081, CEP 81531-990 Curitiba, Paraná, Brazil*
[b] *Laboratório de Química do estado Sólido, CP 19081, CEP 81531-990 Curitiba, Paraná, Brazil*
[c] *Centro de Pesquisa em Química Aplicada (CEPESQ), CP 19081, CEP 81531-990 Curitiba, Paraná, Brazil*

Received 9 July 2007; received in revised form 6 December 2007; accepted 9 December 2007
Available online 23 December 2007

**Abstract**

This paper describes the immobilization of anionic and cationic metalloporphyrins into the nanotubes/nanoscrolls of natural halloysite and investigates the catalytic activity of these novel materials in the oxidation of organic substrates. Two methods for metalloporphyrin immobilization were tested: immobilization under pressure and immobilization under stirring/reflux conditions. The best immobilization rate (100%) was obtained with the anionic iron(III) porphyrin immobilized via the pressurized system. A cationic iron(III) porphyrin was also immobilized into the support with relatively good yields, but no encouraging results were obtained for the immobilization of a neutral iron(III) porphyrin. The obtained materials were characterized by UV–vis and infrared spectroscopies, X-ray diffraction, and transmission electron microscopy. The catalytic activity of a fully immobilized iron(III) porphyrin was evaluated in the oxidation of cyclo-octene, cyclohexane and *n*-heptane, using iodosylbenzene as the oxygen donor. It has been shown that these novel immobilized catalysts are a promising system for selective oxidation reactions.


*Keywords:* Porphyrin; Halloysite; Supported catalyst; Catalysis; Oxidation

## 1. Introduction

Metalloporphyrins are important examples of macrocyclic complexes. Their ability to perform hydrocarbon oxidation under mild conditions has attracted much interest in the last few decades [1–4]. Iron(III) and manganese(III) porphyrins have been the most successful metalloporphyrins used for this purpose [5,6].

Even though very efficient homogeneous metalloporphyrin systems for hydrocarbon hydroxylation and epoxidation have been found, problems such as oxidative catalyst degradation in the presence of inert substrates are challenges that are still to be met for the large-scale use of these complexes. One approach to the mitigation of metalloporphyrin degradation is through their immobilization/encapsulation into supports such as silica [7], zeolites [8], cationic exchanger montmorillonite clay [9], silanized kaolinite [10], intercalated/delaminated kaolinite [11], chrysotile [12,13] and other matrices [14].

Other advantages of metalloporphyrin immobilization include (i) site-isolation of the metal center, which minimizes catalyst self-destruction and metalloporphyrin dimerization; (ii) easy isolation of the heterogeneous catalyst from the reaction media; (iii) possibility of using the catalysts in flow reactors; (iv) facile reuse/recycling of the catalyst, which minimizes environmental impact. The way the metalloporphyrin is attached to the support is extremely important because different binding modes can lead to different selectivities in the oxidation reactions (e.g. regioselectivity).

Selective catalytic materials may result from controlling the formation of either the pore structure of the support or the three-dimensional network of the matrix [15]. In fact, control of particle morphology is one of the major challenges regarding the industrial use of silica. Based on their "unusual" structures and properties, layered materials, fibres

* Corresponding author at: Universidade Federal do Paraná, Departamento de Química, Laboratório de Bioinorgânica e Catálise, CP 19081, CEP 81531-990 Curitiba, Paraná, Brazil. Fax: +55 41 33613186.
*E-mail address:* shirley@quimica.ufpr.br (S. Nakagaki).

1381-1169/$ – see front matter © 2007 Elsevier B.V. All rights reserved.
doi:10.1016/j.molcata.2007.12.009

and open nanotubes/nanoscrolls are potential materials for the immobilization/encapsulation of active metallocomplexes. Upon immobilization, the homogeneous active species is transformed into a heterogeneous catalyst, while its selectivity and high activity are retained. In this context, halloysite, a tubular mineral clay belonging to the same family as kaolinite [16], is a promising support for metalloporphyrin immobilization. The shape of its crystal offers interesting immobilization alternatives, which can takes place at the surface or inside the tubes/scrolls, thus leading to highly active and selective oxidation catalysts.

Halloysite is a mineral clay (1:1, Al:Si) that can be found in some soil in wet tropical and subtropical regions, weathered rocks, and soil generated from volcanic ashes [17,18].

Halloysite can be found in two different forms, namely dehydrated ($Al_2Si_2O_5(OH)_4$: basal distance of 7 Å) and hydrated halloysite ($Al_2Si_2O_5(OH)_4 \cdot 2H_2O$: basal distance of 10 Å). From the morphological point-of-view, halloysite consists typically of nanotubes/nanoscrolls [16,18], but other forms such as the pseudo-spherical and platy shapes have also been reported [17]. The curled crystals originate from the mismatch of the octahedral gibbsite-like sheet and the silica-like sheet, exposing Si–O groups at the outer surface, Al–OH groups at the inner surface, and Al–OH and Si–OH groups at the edges of the material.

Halloysite can easily intercalate water monolayers as well as other organic and inorganic compounds, such as formamide [19] and others [20]. This characteristic of fast intercalation of mineral clays with small organic molecules [17] can be used to distinguish 7 Å kaolinite and 7 Å halloysite in some specific soils.

The immobilization of metallocomplexes in halloysite clay can be performed both inside and outside of the tubes. The immobilization can prevent the molecular aggregation and bimolecular self-destruction reactions, frequent problems observed in homogeneous catalysis, facilitate the recovery and reuse of the catalyst, reduce the cost of material preparation, being very stable chemically and thermally, having good mechanical properties and being based on non-toxic elements (Al and Si). The empty tube having a pre-defined diameter, allowing the entrance of molecules with specific sizes can give shape selectivity to the catalyst. Regioselectivity can also be achieved when only part of the molecule can penetrate the tube and come in contact with the active site, allowing selective reactions, which are not selective in homogeneous media. Crucial aspects to consider when environmentally benign chemical processes for industrial applications are designed and high cost catalysts are used can be summarized in some keywords: improve the catalytic activity of different molecular species such as metalloporphyrins, reduce the cost, facilitate the catalysts separation from the reaction media, allow an easy recycling and disposal of the catalysts after use.

The reactivity and higher cationic exchange capacity of halloysite as compared to kaolinite [21] make the former a potentially useful support for the immobilization of catalytically active molecules. Our research group has recently reported immobilization of both the anionic iron(III) porphyrin $Na_4$[Fe(TDFSPP)Cl] and the neutral iron(III) porphyrin [Fe(TPFPP)]Cl into a tubular kaolinite derived from platelet kaolinite by an intercalation/delamination procedure [11]. We have also described the use of these catalysts in the oxidation of organic compounds [11].

Based on the examples cited above, the present work is aimed at developing a simple method for the preparation of efficient and selective heterogeneous catalysts consisting of metalloporphyrins immobilized into natural halloysite nanotubes/nanoscrolls for hydrocarbon oxidation. Fig. 1 shows the structure of the metalloporphyrins studied in the present work.

## 2. Experimental

### 2.1. Reagents

Chemicals used in this study were of an analytical grade and used without any further treatment. They were purchased from Aldrich, Sigma or Merck. Iodosylbenzene (PhIO) was synthesized by the hydrolysis of iodosylbenzenediacetate [22]. The solid was carefully dried under reduced pressure and kept at 5 °C. The purity was periodically monitored by iodometric titration [23].

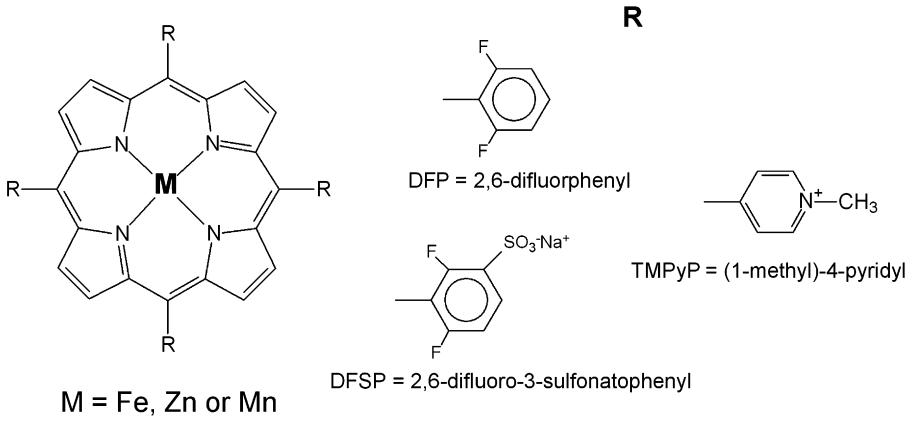


Fig. 1. Structure of the metalloporphyrins used in this study: [Fe(TDFPP)]Cl: [5,10,15,20-tetrakis(2,6-difluorophenyl)porphyrinate iron(III)]chloride, {$Na_4$[M(TDFSPP)]}Cl: [tetrasodium-5,10,15,20-tetrakis(2,6-difluorphenyl-3-sulfonatophenyl)porphyrinate metal M(III)]chloride (M = Fe(III) or Mn(III)). {$Na_4$[Zn(TDFSPP)]}: {[5,10,15,20-tetrakis(2,6-difluorphenyl-3-sulfonatophenyl) porphyrinate zinc(II)]tetrasodium}, [Fe(TMPyP)$Cl_4$]Cl: [5,10,15,20-tetrakis-1-methyl-4-pyridylporphyrinate iron(III) tetrachloride salt]chloride.

The halloysite mineral clay was obtained from Matauri Bay, New Zealand, by Imerys Tableware New Zealand Ltd. Halloysite extracted from Mataury Bay is very pure and it is formed from rhyolite and dacite by low temperature hydrothermal alteration [18].

### 2.2. Porphyrins and metalloporphyrins

The free base porphyrins [$H_2$(TDFPP)] (neutral) and $Na_4$[$H_2$(TDFSPP)] (anionic) and their corresponding Fe(III), Zn(II) and Mn(III) porphyrin complexes were synthesized, purified and characterized following a previously described method [10,24,25]. The tosylate salt of the free base porphyrin [$H_2$(TMPyP)]$^{4+}$ was purchased from Aldrich and the resulting iron(III) porphyrin complex was synthesized, purified and characterized in our laboratory [11–14]. The Soret bands of the metalloporphyrins obtained after the metallation reaction were as follows: [Fe(TDFSPP)]$^{3-}$ (methanol) 392 nm ($\varepsilon = 15 \times 10^3$ L mol$^{-1}$ cm$^{-1}$), [Zn(TDFSPP)]$^{4-}$ (methanol) 418 nm ($\varepsilon = 38 \times 10^4$ L mol$^{-1}$ cm$^{-1}$), [Mn(TDFSPP)]$^{3-}$ (methanol) 460 nm ($\varepsilon = 10 \times 10^4$ L mol$^{-1}$ cm$^{-1}$), [Fe(TMPyP)]$^{5+}$ (methanol) 420 nm ($\varepsilon = 53 \times 10^3$ L mol$^{-1}$ cm$^{-1}$), and [Fe(TDFPP)]$^{1+}$ (chloroform) 410 nm ($\varepsilon = 64 \times 10^3$ L mol$^{-1}$ cm$^{-1}$).[1]

### 2.3. Heterogeneous catalyst preparation

Raw halloysite was characterized by powder X-ray diffraction (XRD), infrared spectroscopy (FTIR), and transmission electron microscopy (TEM). Two immobilization procedures were tested. The first procedure was carried out under solvothermal pressure and, in a typical experiment, the solid metalloporphyrin ($2.5 \times 10^{-3}$ mmol) was transferred to a glass reactor (reactor total volume: 2 mL) containing raw halloysite (100 mg, previously dried under vacuum) and the selected solvent (1.5 mL). Methanol was used as a solvent in the case of the polar metalloporphyrins [Fe(TDFSPP)], [Zn(TDFSPP)], [Mn(TDFSPP)], and [Fe(TMPyP)]; chloroform was chosen for the neutral porphyrin [Fe(TDFPP)]. The glass reactor was sealed and transferred to a Teflon flask placed inside a steel jar. The system was kept in a drying oven at 100 °C for 48 h. After reaction, the suspension was centrifuged, the solution was transferred to a volumetric flask (25 mL), and the solid was washed five times with the respective solvent. The supernatant solutions were analyzed by ultraviolet–visible spectroscopy (UV–vis). The obtained solids were dried at 50 °C and characterized by XRD, FTIR (using KBr pellets), and UV–vis (in Nujol mineral oil).

The second immobilization procedure was carried out under stirring/reflux conditions, at room pressure. For this purpose, raw halloysite (100 mg) was added to the solid metalloporphyrin ($2.5 \times 10^{-3}$ mmol) dissolved in either methanol (5 mL, in the case of the polar metalloporphyrins) or chloroform (5 mL, in the case of the neutral metalloporphyrin) and the resulting mixture was subjected to magnetic stirring and reflux conditions for 48 h. The supernatant solutions were also analyzed by UV–vis.

All the reagents were discarded in an appropriate container for later treatment and reuse, or for final disposal after each experiment.

### 2.4. Cyclo-octene, cyclohexane and n-heptane oxidation by iodosylbenzene (PhIO) catalyzed by a novel supported metalloporphyrin

The polar iron(III) porphyrin [Fe(TDFSPP)] immobilized on raw halloysite by means of the pressurized method was used as catalyst in the oxidation reactions. This solid was designated as Fe-Hallo and this system was chosen because it led to the highest immobilization rate. Catalytic oxidation reactions were carried out in a thermostatic glass reactor (2 mL) equipped with a magnetic stirrer bar. In a typical reaction, Fe-Hallo and iodosylbenzene were suspended in the solvent (0.300 mL dichloromethane/acetonitrile 1:1 v/v). The substrate (cyclooctene, cyclohexane or *n*-heptane) was then added to the reaction mixture, resulting in a constant compound/oxidant/substrate molar ratio of 1:20:2000. The oxidation reaction was carried out for 1 h, under magnetic stirring. Sodium sulfite was added to the reaction mixture to eliminate excess iodosylbenzene and to quench the reaction after the experiment was completed. The reaction products remained in solution. They were separated from the solid catalyst by centrifugation and transferred to a volumetric flask. Then, the solid catalyst was washed several times with dichloromethane and acetonitrile and these washings were transferred to the same volumetric flask containing the reaction products, until the flask was full. The products were analyzed by gas chromatography. Product yields were quantified based on PhIO, using the internal standard method with *n*-octanol (high purity degree, 99.9%) as an internal standard (*n*-octanol $1.0 \times 10^{-2}$ mol L$^{-1}$ in acetonitrile solution). Control reactions were carried out following the same procedure with (a) substrate, (b) substrate + PhIO, and (c) substrate + PhIO + raw halloysite. The parent homogeneous iron(III) porphyrin was tested as catalyst, the procedure employed being similar to that used for the heterogeneous one.

### 2.5. Characterization techniques

For the X-ray diffraction measurements, self-oriented films were placed on neutral glass sample holders. The measurements were performed in the reflection mode using a Shimadzu XRD-6000 diffractometer operating at 40 kV and 40 mA, using Cu Kα radiation (λ = 1.5418 Å) and a dwell time of 1° min$^{-1}$.

FTIR spectra were recorded on a Biorad 3500 GX spectrophotometer in the 400–4000 cm$^{-1}$ range. The KBr pellets were obtained by crushing the solids (1 mg) around spectroscopic grade KBr (100 mg). All the spectra were collected with a resolution of 4 cm$^{-1}$ and accumulation of 32 scans.

UV–vis spectra were recorded in the 200–800 nm range on an HP 8452A Diode Array Spectrophotometer, using a 1-cm path length cell.

[1] Hereafter no mention of charges of metalloporphyrins is made in the text to avoid repetition.

Transmission electron microscopic studies were carried out on suspended powder samples evaporated on 300 mesh copper grids covered with parlodium or amorphous formvar carbon. This was carried out using a JEOL-JEM 1200 equipment operating at 100 kV.

Electron paramagnetic resonance (EPR) measurements were performed using a Bruker ESP 300E spectrometer operating at the X-band (approximately 9.5 GHz), at 293 K or 77 K, using liquid $N_2$.

All the products from the catalytic oxidation reactions were identified using a Shimadzu GC-14B gas chromatograph (flame ionization detector) equipped with a 30-m long and 0.25 mm internal diameter DB-WAX capillary column (J&W Scientific). The oven temperature program used for cyclo-octene and cyclohexane determination was starting at 100 °C, increasing to 150 °C at 10 °C $min^{-1}$ followed by further increase to 200 °C at 50 °C $min^{-1}$ and stabilizing at this temperature for 1 min. For *n*-heptane, the temperature program used was starting at 80 °C, increasing the temperature to 100 °C at 5 °C $min^{-1}$ and stopping for 1 min, increasing the temperature to 200 °C at 10 °C $min^{-1}$ and stabilizing at this temperature for 1 min.

## 3. Results and discussion

Fig. 2 shows the transmission electron micrographs of halloysite of different conditions. Fig. 2(a) and (b) is the raw halloysite, Fig. 2(c) and (d) is that of halloysite on which [Fe(TDFSPP)] was immobilized under the pressurized system (Fe-Hallo) and Fig. 2(e) and (f) is that of halloysite on which [Fe(TDFSPP)] was immobilized under magnetic stirring/reflux conditions. The TEM micrographs showed that the raw halloysite consisted mainly of thick tubes/scrolls ca. 100 nm in diameter and several micrometers in length, thus confirming the high purity of the samples. It may be seen that in most cases, the tubes are still under formation, looking like agglomerates and round crystals due to improper rolling. From the TEM results, it is difficult to observe any change in the surfaces after the immobilization.

Table 1 shows the metalloporphyrin immobilization rates for the two evaluated systems. The supernatant obtained after metalloporphyrin immobilization was analyzed by UV–vis (results not shown). Names were designated to the four solids obtained via the pressurized method, as described in Table 1. The anionic and the cationic metalloporphyrins gave high immobilization rates, while the neutral iron(III) porphyrin immobilization gave none. This result is expected because mineral clays belonging to the kaolinite group have affinity for charged species only. Therefore, only small polar molecules can be directly intercalated into kaolinite and intercalation of non-charged metalloporphyrins is impossible [16].

Halloysite has negative charges on its surface and negative/positive charges at its edges at pH values ranging from 3 to 10 [18]. The surface charges remain practically unaffected with varying pH [26]. With respect to the charges at the edges, the structure of the mineral clay is disrupted and bond cleavages occur at different pH values, thus exposing hydroxyl groups [27]. The charges at the edges are therefore attributed to the protonation/deprotonation of silanol and aluminol groups, which are pH-dependent [26]. In the present study, metalloporphyrin immobilization was accomplished in organic solvents (methanol and chloroform), which hindered the determination of solution pH. The pH of an aqueous suspension of halloysite usually lies between 5 and 6, which is close to the pH of the organic solutions. Therefore, in this discussion, we assume that the pH of the immobilization solution also lies in this range.

In the case of the anionic metalloporphyrins, the aluminol groups were identified as their preferential immobilization sites on the support, which largely occur at the ends of the tube. In the pH ranging from 5 to 6, these sites are protonated and therefore present a positive charge: $Al(OH_2)^+$ [18,27]. Bearing in mind that the isoelectric point of kaolinite and halloysite is around pH 3.0, the silanol groups at the edge must be completely deprotonated at pH higher than 3, $SiO^-$ being the predominant species in the product [26]. The anionic iron(III) porphyrin (Fe-Hallo) was more efficiently immobilized compared to Zn-Hallo and Mn-Hallo. In fact, the immobilization rates of Zn-Hallo and Mn-Hallo were lower than that of Fe-Hallo. One explanation for this behavior is the higher acidity of $Fe^{3+}$than that of $Mn^{3+}$ and $Zn^{2+}$. The $Fe^{3+}$ metallic center increases the solution acidity, whereby the number of protonated aluminol sites also increases. This higher acidity allows immobilization of a large amount of iron(III) porphyrin compared to that of other metalloporphyrins.

As for the cationic metalloporphyrin (Py-Hallo), its immobilization can occur through the $SiO^-$ groups or/and on the surface of the clay. The negatively charged surface in the halloysite can be the result of replacing structural $Si^{4+}$ with $Fe^{3+}$ or $Al^{3+}$ [18,21]. In fact, the presence of $Fe^{3+}$ was confirmed in this clay by EPR. Fig. 3 shows the EPR spectrum of raw halloysite, where the presence of high-spin $Fe^{3+}$ in the rhombic symmetry is clear from the lines present at $g = 8.0$, 4.3, and 2.0 [12]. The intense iron(III) signals in the mineral clay makes the characterization of the immobilized metalloporphyrins by this technique impossible.

Finally, no immobilization was observed for the neutral iron(III) porphyrin, which suggests absence of entrapped metalloporphyrin inside the nanotubes/nanoscrolls, and reinforces the idea that the immobilization probably occurs via ionic interaction between the halloysite charges and the metalloporphyrin polar groups.

The pressurized system has led to higher immobilization rates than the stirring/reflux method. This is because the metalloporphyrin and halloysite come into closer contact during the former process, which results in more effective immobilization. In the stirring/reflux process, the system is open and water molecules can be adsorbed by the catalyst and the clay, which could deactivate the immobilization sites.

Fig. 4 shows the FTIR spectra of raw halloysite (a), Fe-Hallo (b), Zn-Hallo (c), Mn-Hallo (d), and Py-Hallo (e). The spectrum of raw halloysite displays two intense characteristic bands at 3698 $cm^{-1}$ and 3622 $cm^{-1}$ [21,28], which correspond to the O–H group vibration and to the surface hydroxyl groups, respectively. The band due to water deformation is observed at 1634 $cm^{-1}$ [21], the band attributed to Si–O group appears at 1036 $cm^{-1}$, and the band relative to the Al–OH group can be

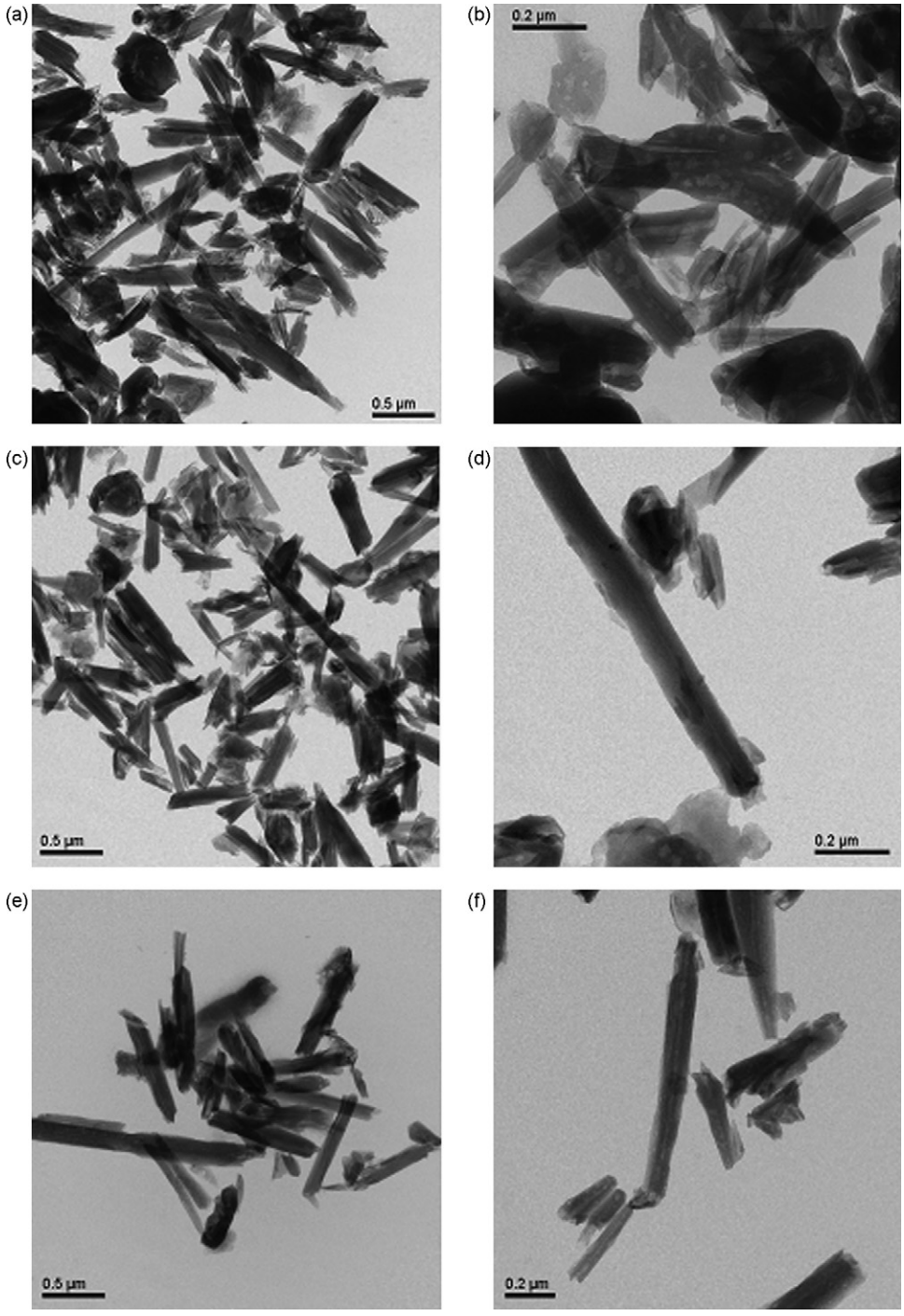


Fig. 2. Transmission electron micrographs of raw halloysite (a and b), Fe-Hallo (c and d) and $[Fe(TDFSPP)]^{3-}$ immobilized into halloysite by magnetic stirring and reflux (e and f).

seen at 912 $cm^{-1}$ [18]. In all immobilized metalloporphyrins (Fe-Hallo, Zn-Hallo, Mn-Hallo and Py-Hallo), only the intense bands of the support are observed. Based on the low concentration of the adsorbate in the support, the characteristic vibration bands of the groups present on the metalloporphyrins are not observed.

As the proposed immobilization mechanism suggests that the interaction of the metalloporphyrin with the edge aluminol groups take place and the concentration of the immobilized species is very low, a study of the band intensities in the region of 3000–4000 $cm^{-1}$ would be merely speculative.

Fig. 5 shows the powder X-ray diffraction patterns of raw halloysite (Fig. 5(a)), Fe-Hallo (Fig. 5(b)), Zn-Hallo (Fig. 5(c)), Mn-Hallo (Fig. 5(d)), and Py-Hallo (Fig. 5(e)). Raw halloysite presents a series of diffraction peaks with a basal distance of 7.4 Å [17]. The characteristic basal diffraction peak of hydrated halloysite at 10.0 Å is not observed, which is expected for the fully dehydrated halloysite extracted from Matauri Bay [29].

Table 1
Metalloporphyrin immobilization into raw halloysite

| Metalloporphyrin | Immobilization rate (%) | Immobilization system | Denomination | Concentration (mol $g^{-1}$)[a] |
|---|---|---|---|---|
| $[Fe(TDFSPP)]^{3-}$ | 100 | Pressure | Fe-Hallo | $1.59 \times 10^{-5}$ |
| $[Zn(TDFSPP)]^{4-}$ | 47 | | Zn-Hallo | $7.25 \times 10^{-6}$ |
| $[Mn(TDFSPP)]^{3-}$ | 43 | | Mn-Hallo | $7.38 \times 10^{-6}$ |
| $[Fe(TMPyP)]^{5+}$ | 98 | | Py-Hallo | $2.11 \times 10^{-5}$ |
| $[Fe(TDFPP)]^{1+}$ | 0 | | – | – |
| $[Fe(TDFSPP)]^{3-}$ | 80 | Stirring/reflux | – | $1.27 \times 10^{-5}$ |
| $[Zn(TDFSPP)]^{4-}$ | 35 | | – | $5.57 \times 10^{-6}$ |
| $[Mn(TDFSPP)]^{3-}$ | 38 | | – | $6.23 \times 10^{-6}$ |
| $[Fe(TMPyP)]^{5+}$ | 92 | | – | $1.97 \times 10^{-5}$ |
| $[Fe(TDFPP)]^{1+}$ | 0 | | – | – |

[a] Concentration of metalloporphyrin (mol) in halloysite (1.00 g).

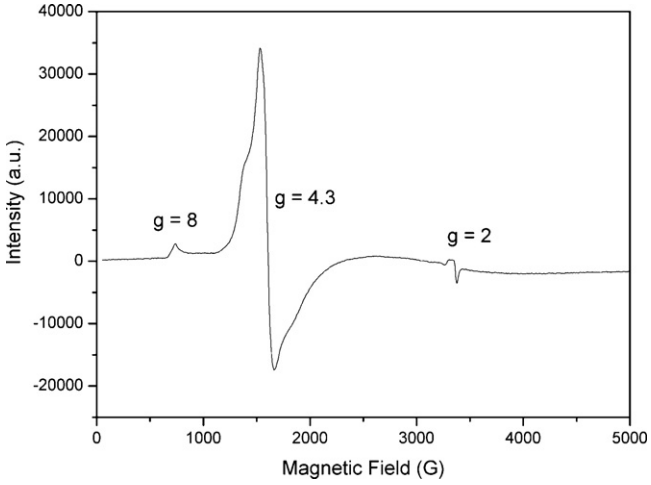


Fig. 3. EPR spectrum of raw halloysite at 77 K.

The samples containing metalloporphyrin (Fe-Hallo, Zn-Hallo, Mn-Hallo and Py-Hallo) display the basal diffraction peaks in the same positions as those of the raw halloysite, suggesting that immobilization of the metalloporphyrin takes place on the surface and at the edges of the support. No other crystalline impurity was detected by powder X-ray diffraction, thus confirming the high purity of the sample both before and after the immobilization process.

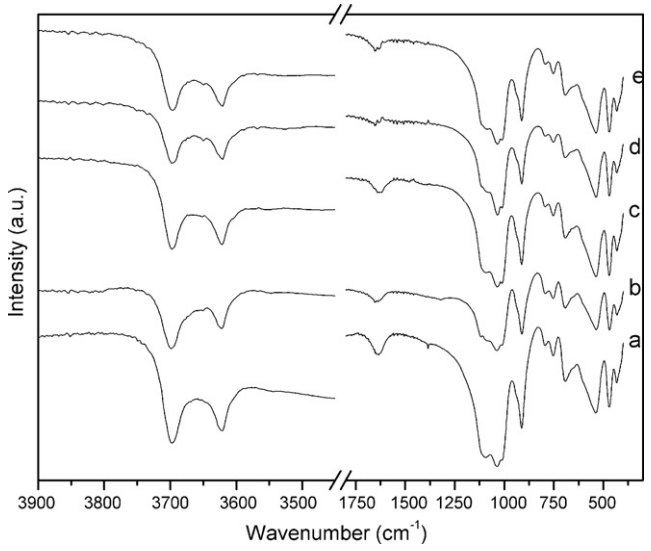


Fig. 4. FTIR spectra of raw halloysite (a), Fe-Hallo (b), Zn-Hallo (c), Mn-Hallo (d), and Py-Hallo (e).

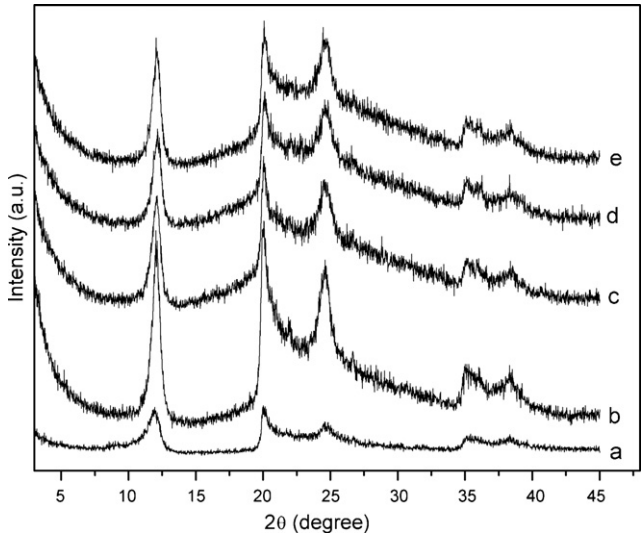


Fig. 5. Powder X-ray diffraction patterns of raw halloysite (a), Fe-Hallo (b), Zn-Hallo (c), Mn-Hallo (d), and Py-Hallo (e).

The presence of the metalloporphyrins in the Fe-Hallo, Zn-Hallo, Mn-Hallo and Py-Hallo solids was confirmed by the UV–vis spectra of the solids in Nujol mineral oil (Fig. 6). The metalloporphyrin Soret bands were identified at 412 nm for Fe-Hallo, 424 nm for Zn-Hallo, 468 nm for Mn-Hallo, and 432 nm for Py-Hallo, as shown in Fig. 6(a–e), respectively. Fig. 6(a) shows the spectrum of raw halloysite, where no peaks are present. This suggests that no demetallation (characterized by a blue shift of the Soret band typical of the presence of a significant amount of free base porphyrin [13]) or significant metallic ion exchange between the metallocomplex and the support occurred during the preparation process. The Soret peaks showed red-shift compared to those of the metalloporphyrins in solution (methanol): 392 nm for [Fe(TDFSPP)], 418 nm for [Zn(TDFSPP)], 460 nm for [Mn(TDFSPP)] and 420 nm for [Fe(TMPyP)]. Similar behavior has been previously observed [12] for metalloporphyrins immobilized onto different inorganic supports [10], and it has been attributed to steric constraints of

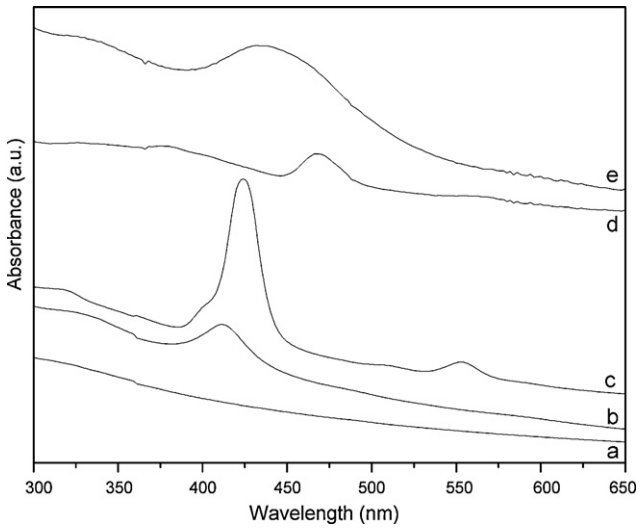


Fig. 6. UV–vis spectra of solid raw halloysite (a), Fe-Hallo (b), Zn-Hallo (c), Mn-Hallo (d), and Py-Hallo (e).

the support, which substantially modify the metalloporphyrin structure in these supported catalysts [12].

The catalytic activities of both the anionic iron(III) porphyrin [Fe(TDFSPP)] (homogeneous catalyst) and the corresponding supported catalyst, Fe-Hallo (heterogeneous catalysis) were investigated in the oxidation of three organic substrates namely the cyclic hydrocarbons cyclo-octene and cyclohexane and the linear alkane *n*-heptane. The results are given in Tables 2 and 3, for cyclohexane products and *n*-heptane products, respectively. For comparison, the results recently published by the authors for the same metalloporphyrin [Fe(TDFSPP)] immobilized into synthetic halloysite-like tubes obtained from intercalated/delaminated kaolinite are also included [11].

Cyclo-octene was the first substrate used for the evaluation of the catalytic activity of Fe-Hallo, using iodosylbenzene as an oxidant. The catalytic results are promising since cyclo-octene oxide has been obtained with a yield of 99%, which is better than that achieved (68%) with the homogeneous catalyst. It has been frequently reported that the catalytic activity of the metalloporphyrin is reduced upon immobilization because the access of both the substrate and the oxidant to the active site is limited; in the present study, however, the catalytic site has been exposed due to the distortion of the iron(III) porphyrin structure. Another positive factor which has been achieved in the present solid catalyst is the isolation of the iron(III) porphyrin complex active center through the low clay coverage with the catalyst.

Table 2
Cyclohexane oxidation by PhIO catalyzed by an anionic iron(III) porphyrin in different media[a]

| Catalyst | Alcohol yield (%)[b] | Ketone yield (%)[b] | Alcohol/ ketone | Run |
|---|---|---|---|---|
| Fe-Hallo | 39 | 3 | 13 | 1 |
| $[Fe(TDFSPP)]^{3-}$ | 19 | 7 | 3 | 2 |
| Fe-Kao-Hallo | 28 | – | 28 | 3 |
| Raw halloysite | Trace | Trace | – | 4 |

[a] Conditions: catalyst:oxidant:cyclohexane molar ratio = 1:20:2000; reactions were carried out in a dichloromethane/acetonitrile 1:1 mixture (v/v) at room temperature, under argon. Homogeneous catalyses were performed under conditions identical to those employed for the heterogeneous catalyses.

[b] Yields based on starting PhIO (it was assumed that 2 mol of iodosylbenzene were necessary for ketone formation). Fe-Hallo: [Fe(TDFSPP)] immobilized on raw halloysite by means of the pressurized method. $[Fe(TDFSPP)]^{3-}$: homogeneous catalysis. Fe-Kao-Hallo: [Fe(TDFSPP)] immobilized on synthetic halloysite-like nanotubes [11].

Cyclohexane oxidation by iodosylbenzene in the presence of metalloporphyrins generally produces cyclohexanol and cyclohexanone as the major products, making them good biomimetic models of cytochrome P-450. Table 2 shows that the homogeneous iron(III) porphyrin used in this work gives low yields of oxidation product (homogeneous catalysis—run 2), which can be attributed to the poor solubility of this anionic iron(III) porphyrin in the solvent mixture used in the catalytic reactions, as previously reported [11].

These insolubility problems were minimized by immobilizing the anionic iron(III) porphyrin into raw halloysite (Fe-Hallo—run 1) or into synthetic halloysite-like nanotubes (Fe-Kao-Hallo—run 3 [11]). Compared to the homogeneous catalyst, catalyst efficiency and the alcohol production rate were higher with the heterogeneous iron(III) porphyrins.

The catalyst Fe-Hallo led to higher alcohol yields than those obtained with Fe-Kao-Hallo. But a small amount of ketone was also observed in the case of the former solid. Therefore, Fe-Hallo is less selective for alcohol than Fe-Kao-Hallo. The higher product yields obtained with Fe-Hallo can be explained by the different metalloporphyrin immobilization modes on the supports. The metalloporphyrin is preferentially immobilized at the edges of raw halloysite. Though a small amount of the metalloporphyrin is immobilized at the edges in synthetic halloysite-like material, the remaining metalloporphyrin is probably immobilized inside the nanotubes. Entrapment of the metalloporphyrin in this case is possible because the rolling of the nanotubes has been performed in the presence of the metallocomplex. We suppose that in Fe-Hallo there are more active sites available for substrate oxidation, whereas in the case of Fe-Kao-Hallo, part of the catalytic sites are located inside the tubes, hindering the access of the cyclic substrates to the iron(III) porphyrin difficult.

Metalloporphyrins and other transition metal complexes, either in solution or immobilized, are frequently used in the oxidation of linear alkanes such as *n*-heptane [10,11,30–32]. The regioselectivity of the *n*-heptane oxidation process is essentially thermodynamically controlled when metalloporphyrins are used as catalysts in the absence of steric constraints [33], so the observed product distribution is consistent with the formation of a radical intermediate species obtained via hydrogen atom abstraction [34]. In other words, the observed product ratio depends on the strength of the alkane C–H bonds, with oxidation taking place preferentially at tertiary and secondary carbons instead of primary carbons [31].

However, in the presence of steric constraints posed by the support [10] or by the porphyrin structure itself [35], the efficiency and selectivity of linear alkane oxidation can be changed. This was in fact observed for the anionic iron(III) porphyrin in solution and immobilized into halloysite. The yields of *n*-heptane oxidation products (Table 3) exhibited similar behavior

Table 3
*n*-Heptane oxidation with PhIO catalyzed by an anionic iron(III) porphyrin in different media[a]

| Catalyst | Alcohol yield (%)[b,c] | Ketone yield (%)[b,c] | Alcohol/ketone | Regioselectivity (%)[d] | | | | Run |
|---|---|---|---|---|---|---|---|---|
| | | | | C-2 | | C-3 | | |
| | | | | ol | one | ol | one | |
| Fe-Hallo | 55 | 8 | 7 | 60 | – | 40 | 100 | 5 |
| $[Fe(TDFSPP)]^{3-}$ | 31 | 12 | 3 | 100 | – | – | 100 | 6 |
| Fe-Kao-Hallo | 71 | 4 | 18 | 61 | – | 39 | 100 | 7 |
| Raw halloysite | – | – | – | – | – | – | – | 8 |

[a] Conditions: catalyst:oxidant:cyclohexane molar ratio = 1:20:2000; reactions were carried out in a dichloromethane/acetonitrile 1:1 mixture (v/v) at room temperature, under argon. Homogeneous catalyses were performed under conditions identical to those employed for the heterogeneous catalyses.
[b] Yields based on starting PhIO (it was assumed that 2 mol of iodosylbenzene were necessary for ketone formation).
[c] C-2 and C-3 heptane products of oxidation (alcohol and ketone). The yield for products corresponding to the C-1 and C-4 heptane positions was not observed.
[d] Relative proportions of products (%) at positions C-2 and C-3 of heptane. The positions C-1 and C-4 of heptane did not present product yields. ol = heptanol and one = heptanone.
Fe-Hallo: [Fe(TDFSPP)] immobilized on raw halloysite by means of the pressurized method. $[Fe(TDFSPP)]^{3-}$: homogeneous catalysis. Fe-Kao-Hallo: [Fe(TDFSPP)] immobilized on synthetic halloysite-like nanotubes [11].

to that observed for the cyclohexane oxidation; homogeneous [Fe(TDFSPP)] converted less substrate to alcohol compared to Fe-Hallo. In addition, oxidation preferentially occurred at carbons 2 and 3. No quantitative yields below 2% for products from C-1 or C-4 oxidation were observed, contrary to what would be expected for the oxidation of this linear alkane.

The charged [Fe(TDFSPP)] (run 6) was highly selective for alcohol formation at the C-2 position and for ketone formation at the C-3 position (Table 3, regioselectivity % data). Metalloporphyrins do not normally discriminate between secondary sites (C-2 and C-3), with the product ratio 2-heptanol/3-heptanol being close to 1. This was in fact observed in the case of the unhindered metallotetraphenylporphyrin [36]. But the presence of the sulfonate groups at the meta positions of the meso phenyl rings of the porphyrin in [Fe(TDFSPP)] and their negative charges probably make substrate access to the metal center difficult. So this iron(III) porphyrin poses more steric hindrance to the approach of the secondary C-3 site of heptane, but once 3-heptanol is produced, this iron(III) porphyrin is capable of converting it into 3-heptanone.

The catalytic behavior of the anionic iron(III) porphyrin changes upon immobilization. The catalytic efficiency for hydroxylation appears to arise from controlling the access of the substrate to the active site or from controlling the access of iodosylbenzene to generate the oxidizing species. Compared to the homogeneous iron(III) porphyrin, Fe-Hallo (run 5) and Fe-Kao-Hallo (run 7) led to increased alcohol yields and decreased ketone yields. Furthermore, the solid catalysts were more selective for alcohol than the homogeneous one. Although the total product yields obtained with Fe-Hallo (71% = 55 (alcohol) + 8 × 2 (ketone)) and Fe-Kao-Hallo (79% = 71 (alcohol) + 4 × 2 (ketone)) were similar, the selectivity for alcohol over Fe-Kao-Hallo was higher. This behavior, as explained in the case of cyclohexane oxidation, can be attributed to the different ways the anionic iron(III) porphyrin is immobilized on the supports. In the case of Fe-Hallo, the catalyst is immobilized at the edges, making a closer contact between the substrate and the generated alcohol molecules possible, which results in higher ketone yields. As for Fe-Kao-Hallo, some molecules of [Fe(TDFSPP)] can be immobilized inside the nanotubes, and *n*-heptane, a linear alkane, can be inserted into the nanotubes and be oxidized to the alcohol, but the new polar molecule formed therein can somehow be removed from the interior of the support before being further oxidized to the ketone. Because in the case of Fe-Kao-Hallo a lower amount of metalloporphyrin is immobilized at the edges, a lower amount of alcohol molecules was oxidized to the corresponding ketone.

Fe-Hallo and Fe-Kao-Hallo led to similar alcohol yields at positions C-2 and C-3, at the rates comparable to those observed for iron(III) porphyrins in general [36]. No [Fe(TDFSPP)] leaching was observed during the heterogeneous catalytic reaction, to justify the drastic catalytic behavior changes observed ongoing from the homogeneous catalyst to the heterogeneous ones. It is therefore reasonable to assume that the immobilization of [Fe(TDFSPP)] occurs through the strong charge interaction between the solid support and the iron(III) porphyrin sulfonate groups. Such interaction should expose the catalytic active site, facilitating greater of C-2 compared to that of C-3.

Finally, no oxidation products arising from cyclohexane or *n*-heptane were detected in the presence of the raw halloysite without iron(III) porphyrin (runs 4 (Table 2) and 8 (Table 3)). This shows that iron(III) porphyrin really mediates oxygen atom transfer from iodosylbenzene to the substrates. In the case of cyclo-octene the behavior was different (not shown); raw halloysite gives 20% epoxide yield and the reaction of the substrate with iodosylbenzene gives 10% epoxide yield, performed in the same conditions. This is possible because cyclo-octene is easily oxidized even in the absence of a catalyst.

## 4. Conclusions

Anionic and cationic metalloporphyrin immobilization into the natural nanotubes/nanoscrolls of halloysite is reported here for the first time. Investigation of different immobilization strategies and the use of different metalloporphyrins enabled the establishment of an efficient method for [Fe(TDFSPP)] immobilization, using a closed vessel and autogeneous pressure. As metalloporphyrin immobilization occurs at the edges/surfaces

of the halloysite nanotubes, the catalyst structure is retained, as observed in several analytical techniques. The presence of the metalloporphyrin on the clay was attested by solid state UV–vis techniques and evaluation of the catalytic activity of the solid.

Halloysite is a very versatile tubular aluminosilicate, having high surface areas, being low-priced and broadly available especially in tropical countries and having reactive inner tube surface. As halloysite is from natural origin and rolled kaolinite [11] is produced by a laborious intercalation reaction mechanism, the reason to use halloysite instead of nanoscroll of kaolinite is in our perception obvious. On the other hand, the catalytic activity is similar when the same metalloporphyrin is used, investigation of the catalytic activity of [Fe(TDFSPP)] immobilized into halloysite in the oxidation of alkanes has shown that this novel catalyst is highly efficient and highly selective for the alcohol as observed to the rolled kaolinite [11]. Therefore, very common and abundantly available materials, especially those occurring in the form of nanotubes, nanofibres or nanolayers, can be used for technological purposes. Other fibrous materials are under investigation in our laboratory and their activities will be presented in a forthcoming publication.

## Acknowledgements

The authors thank Conselho Nacional de Desenvolvimento Científico e Tecnológico (CNPq), Coordenação de Aperfeiçoamento de Pessoal de Nível Superior (CAPES), Fundação Araucária (FA-PR), Fundação da Universidade Federal do Paraná (FUNPAR), and Universidade Federal do Paraná (UFPR) for financial support. They also thank the Centro de Microscopia Eletrônica da UFPR (Rosangela Borges Freitas) for the TEM analyses, Dr. José Eduardo Ferreira da Costa Gardolinski for supplying the halloysite sample and Prof. Kestur Gundappa Satyanarayana for reading the manuscript, critical comments and helpful suggestions including English language.

## References

[1] A.A. El-Awady, P.C. Wilkins, R.G. Wilkins, Inorg. Chem. 24 (1985) 2053.
[2] D. Mansuy, Coordin. Chem. Rev. 125 (1993) 129.
[3] F. Bedioui, Coordin. Chem. Rev. 144 (1995) 39.
[4] J. Haber, L. Matachowski, K. Pamin, J. Poltowicz, J. Mol. Catal. A: Chem. 198 (2003) 215.
[5] J.R. Lindsay Smith, Metalloporphyrins in Catalytic Oxidations, Marcel Dekker Inc., New York, 1994, p. 325.
[6] T. Aida, S. Inoue, in: K.M. Kadish, K.M. Smith, R. Guilard (Eds.), The Porphyrin Handbook, Academic Press, San Diego, 1999, p. 133.
[7] Y. Iamamoto, Y.M. Idemori, S. Nakagaki, J. Mol. Catal. A: Chem. 99 (1985) 187.
[8] S. Nakagaki, C.R. Xavier, A.J. Wosniak, A.S. Mangrich, F. Wypych, M.P. Cantão, I. Denicoló, L.T. Kubota, J. Colloid Surf. A 168 (2000) 261.
[9] A.M. Machado, F. Wypych, S.M. Drechsel, S. Nakagaki, J. Colloid Interf. Sci. 254 (2002) 158.
[10] S. Nakagaki, F.L. Benedito, F. Wypych, J. Mol. Catal. A: Chem. 217 (2004) 121.
[11] S. Nakagaki, G.S. Machado, M. Halma, A.A.S. Marangon, K.A.D.F. Castro, N. Mattoso, F. Wypych, J. Catal. 242 (2006) 110.
[12] M. Halma, A. Bail, F. Wypych, S. Nakagaki, J. Mol. Catal. A: Chem. 243 (2006) 44.
[13] S. Nakagaki, K.A.D.F. Castro, G.S. Machado, M. Halma, S.M. Drechsel, F. Wypych, J. Braz. Chem. Soc. 17 (2006) 1672.
[14] S. Nakagaki, F. Wypych, M. Halma, F.L. Benedito, G.R. Friedermann, A. Bail, G.S. Machado, S.M. Drechsel, Met. Mater. Proc. 17 (2005) 363.
[15] D.C. de Oliveira, H.C. Sacco, O.R. Nascimento, Y. Iamamoto, K.J. Ciuffi, J. Non-Cryst. Solids 284 (2001) 27.
[16] J.E. Gardolinski, H.P. Martins, F. Wypych, Q. Nova 26 (2003) 30.
[17] E. Joussein, S. Petit, B. Delvaux, Appl. Clay Sci. 35 (2007) 17.
[18] B.K.G. Theng, M. Russel, G.J. Churchman, R.L. Parfitt, Clay Clay Miner. 30 (1982) 143.
[19] G.J. Churchman, Clay Clay Miner. 38 (1990) 591.
[20] E. Joussein, S. Petit, J. Churchman, B. Theng, D. Righi, B. Delvaux, Clay Miner. 40 (2005) 383.
[21] G. Tari, I. Bobos, C.S.F. Gomes, J.M.F. Ferreira, J. Colloids Interf. Sci. 210 (1999) 360.
[22] J.G. Sharefkin, H. Saltzmann, Org. Synth. 43 (1963) 62.
[23] J. Lucas, E.R. Kennedy, M.W. Forno, Org. Synth. 43 (1963) 483.
[24] J.S. Lindsey, J. Org. Chem. 54 (1987) 827.
[25] A. Adler, F.R. Longo, J. Am. Chem. Soc. 86 (1964) 3145.
[26] K. Itami, H. Fujitani, Colloids Surf. A. 265 (2005) 55.
[27] B. Braggs, D. Fornasiero, J. Ralston, R.S. Smart, Clay Clay Miner. 42 (1994) 123.
[28] P. Adamo, P. Violante, M.J. Wilson, Geoderma 99 (2001) 295.
[29] A.C.V. Coelho, P.S. Santos, H.S. Santos, Q. Nova 30 (2007) 146.
[30] W. Nam, Y.M. Goh, Y.J. Lee, M.H. Lim, C. Kim, Inorg. Chem. 38 (1999) 3238.
[31] J.M. Thomas, R. Raja, G. Sankar, R.G. Bell, Acc. Chem. Res. 34 (2001) 191.
[32] K.S. Suslick, P. Bhyrappa, J.H. Chou, M.E. Kosal, S. Nakagaki, D.W. Smithenry, S.R. Wilson, Acc. Chem. Res. 38 (2005) 283.
[33] K.S. Suslick, S. Van Deusen, Jeffries, in: J.-M. Lehn (Ed.), Comprehensive Supramolecular Chemistry, Elsevier Science Ltd., Oxford, 1996 (Chapter 5).
[34] J.T. Groves, W.J. Kruper, R.C. Haushalter, J. Am. Chem. Soc. 102 (1980) 6375.
[35] K.S. Suslick, B. Cook, M. Fox, J. Chem. Soc., Chem. Commun. (1980) 580.
[36] C.A. Tolman, J.D. Druliner, M.J. Nappa, N. Herron, in: C.L. Hill (Ed.), Activation and Funcionalization of Alkanes, Wiley, New York, 1989, p. 303 (Chapter 10).